J Therm Anal Calorim (2016) 124:1511–1518
DOI 10.1007/s10973-016-5276-2

Experimental thermal behavior response of paraffin wax as storage unit

J. P. Hadiya[1,3] · Ajit Kumar N. Shukla[2]

Received: 2 July 2015 / Accepted: 16 January 2016 / Published online: 3 February 2016

Abstract The paper presents experimental thermal behavior of paraffin wax as phase change material (PCM) using shell and tube with four-pass heat exchanger unit of 1 MJ storage unit under different flow rates. Thermal energy storage unit is constructed to study the performance of commercial grade paraffin white wax as energy storage material. The heat exchanger is constructed to obtain realistic energy storage behavior during charging and discharging cycle. The water is used as heat transfer fluid (HTF) to supply and absorb heat from PCM and to calculate energy stored. The charging and discharging experiments are carried out at constant inlet fluid temperature and constant pressure to observe the effects of flow rate of HTF on the performance of the storage unit at five different flow rates. The result shows that the charging time was in the range 195–310 min while discharging time in the range 80–38 min for change in flow rate from 35 to 75 LPH. The charging as well as discharging cycle time decreases with increase in mass flow rate of HTF, fall in cycle time during discharge is around three times faster than charging, and the same is attributed to fissure crack developed in the lump mass. Increase in flow rate decreases the heat storage.

Keywords Latent heat energy storage · Phase change material · Paraffin wax · Shell and tube storage unit · Experimental thermal behavior of paraffin wax

List of symbols

c	Specific heat (kJ kg^{-1} K^{-1})
f	Function
HTF	Heat transfer fluid
L	Latent heat of fusion (kJ kg^{-1})
LPH	Liter per hour
m	Mass flow rate (kg s^{-1})
M	Total mass of PCM (kg)
PCM	Phase change material
Q	Heat transfer (kJ)
$\dot{Q}$	Heat transfer rate (kJ s^{-1})
R	Correlation coefficient
T	Temperature (°C)
TC	Thermocouple
TES	Thermal energy storage
t	Time (s)
U	Uncertainty (%)
V	Volume of PCM (m^3)

Greek symbols

η	Efficiency

Subscripts

A	Available
f	Final
i	Initial
m	Melting point

✉ J. P. Hadiya
jayant_hadiya@yahoo.co.in

Ajit Kumar N. Shukla
ajit.shukla@rku.ac.in

[1] Research Scholar, Gujarat Technological University, Chandkheda, Ahmedabad 382424, Gujarat, India

[2] School of Engineering, R K University, Bhavnagar Highway, Kasturbadham, Rajkot 360020, Gujarat, India

[3] Mechanical Engineering Department, Birla Vishvakarma Mahavidyalaya Engineering Collage, Vallabhvidyanagar, Anand, Gujarat 388120, India

w Water
wi Water inlet
wo Water outlet

Introduction

As solar energy is an intermittent energy source, there is a mismatch between the energy supply and energy demand. It is necessary to store energy during sunshine hour and supply this stored energy during night or during cloudy weather. Thermal energy storage system is the one of the options to store energy in order to reduce the gap between the demand and supply.

There are two main methods of thermal energy storage (TES) as sensible and latent heat storage [1]. The material which changes phase while storing large energy is called phase change material (PCM). It is gaining a greater attention due to advantages of high storage density and nearly constant thermal energy [2].

Major applications of PCMs are as heat storage medium of solar energy system, as thermal energy storage for off-peak demand in power generation unit, and building applications [3]. Tyagi et al. [4] carried out the experimental study and performance analysis of a solar air heater with and without PCM, viz. paraffin wax and hytherm oil, and found that the output temperature and efficiency in case with TES is higher than that without TES. Jeon et al. [5] reviewed the development of available latent heat thermal energy storage technologies and discussed PCM application methods for residential building using radiant floor heating systems with the goal of reducing energy consumption. Abidi et al. [2], Yuan et al. [6], Liu et al. [7], and Jankowski et al. [8] reviewed PCMs for air conditioning systems, fatty acid PCMs, thermal performance enhancement techniques for high-temperature PCMs, and PCMs for vehicle component thermal buffering, respectively. Harikrishnan et al. [9] investigated thermal and heat transfer characteristics of the newly prepared composite phase change material, viz paraffin and hybrid nanomaterials (50 % CuO–50 % TiO_2), for solar heating systems. It showed heating and cooling rates of composite PCMs are faster due to the dispersion of hybrid nanomaterials.

There are number of PCMs available, and researchers have analyzed performance of PCMs. Rathod et al. [10] reviewed the thermal stability of different groups of PCMs. Min Li and Zhishen Wu [11] studied the effect of the amount of graphite thermal properties of the graphite/*n*-docosane composite PCM and reported the rate of heat storage/release, and the thermal conductivity increased with an increase in the amount of graphite, but the latent heat of the composite PCM decreased with the increase in the amount of graphite. Jeong et al. [12] prepared shape-stabilized phase change materials (SSPCMs) like hexadecane, octadecane, and paraffin and experimentally found their properties like latent heat capacity, and melting points. The characteristics of SSPCMs were determined using SEM, DSC, FTIR, TG, TCi, and energy simulation. Parameshwaran et al. [13] investigated the thermal properties of new silver nano-based organic ester phase change material in terms of latent heat capacity, thermal conductivity, and heat storage and release capabilities experimentally. It reports dispersion of silver nanoparticles into PCM, reduces degree of supercooling, reduces cooling and melting time, and increases thermal conductivity, whereas latent heat capacities decrease. Wang et al. [14] experimentally investigated the thermal conductivity and energy storage of composite PCM, viz. paraffin and micron-size graphite flakes. It shows there is negligible change in the latent heat capacity, the melting temperature, and the freezing temperature, but thermal conductivity increases with increasing the mass fraction of the micron-size graphite flakes. Anghel et al. [15] investigated phase-transition temperatures, latent heat, and heat capacity at constant pressure, density, and thermal conductivity of three phase change paraffinic materials. It reports composite containing ceresin component shows the lowest latent heat value around 144 kJ/kg and the highest thermal conductivity of 0.46 W/m–K among the three PCMs. Murray et al. [16] designed latent heat energy storage unit for domestic hot water solar thermal system in Halifax. They have used lauric acid as PCM in the storage unit.

However, selection of PCMs is critical meeting specific requirements of applications. The commonly used PCMs in solar heat storage are fatty acids, paraffin, and hydrates [17]. Paraffin wax as a PCM is an attractive material for heat storage applications since it has high latent heat storage capacities over a narrow temperature range [18]. Paraffin waxes are cheap, ecologically harmless, and non-toxic. Benmansour et al. [19] investigated numerically and experimentally the performance of encapsulated paraffin wax as PCM with air as working fluid. They developed mathematical model which is validated by experimental work. Groulx et al. [20] modeled circular fins single pipe and shell paraffin wax heat storage performance using COSMOL multi-physics.

PCMs as a thermal energy storage is topic in research for the last 20 years due to limited theoretical information and little experimental works which are limited to laboratories. Therefore, there is a need for realistic experimental investigation of PCMs for solar energy systems so that it can be incorporated with solar energy system. The works experimentally investigate the thermal behavior of commercial grade paraffin white wax (as PCM) using small shell and tube heat exchanger storage unit having four pass. The experimental work report performance parameters

effect of fluid flow rate during melting; called charging and solidification; called discharging of PCM developing the characteristic equations using experimental results. This relationship is henceforth available for use to scale up the project.

Heat transfer during the melting and solidification of PCM

Heat released by water while flowing through the pipe

$$\dot{Q}_{\mathrm{w}} = m_{\mathrm{w}} c_{\mathrm{w}} (T_{\mathrm{wi}} - T_{\mathrm{wo}}), kJs^{-1} \quad (1)$$

Heat absorbed (stored) by PCM during heating

$$Q_{\mathrm{PCM}} = M_{\mathrm{PCM}} c_{\mathrm{PCM}} (T_{\mathrm{m}} - T_{\mathrm{i}}) + M_{\mathrm{PCM}} L_{\mathrm{PCM}} + M_{\mathrm{PCM}} c_{\mathrm{PCM}} (T_{\mathrm{f}} - T_{\mathrm{m}}), kJ \quad [1] \quad (2)$$

Melting (charging) or solidification (discharging) time

$$t = \frac{Q_{\mathrm{PCM}}}{Q_{\mathrm{w}}}, s \quad (3)$$

Heat available

$$Q_{\mathrm{A}} = Q_{\mathrm{w}} \cdot t, kJ \quad (4)$$

Storage efficiency given by

$$\eta = \frac{Q_{\mathrm{PCM}}}{Q_{\mathrm{A}}} \quad [21] \quad (5)$$

Experimental investigation

Experimental setup

The schematic diagram of the experimental setup is shown in Fig. 1. An acrylic cylindrical container (178 mm long and 180 mm inner diameter) as storage tank is used to analyze the performance of phase change material energy storage system. This tank is composed of inner copper pipe (25.4 mm inner diameter and 1 mm thickness) as shown in Fig. 2. The copper pipe has four passes inside the storage tank. The one end of copper pipe is connected with hot water bath and other end to water sink with help of insulated flexible pipes. The spaces between inner copper tube and acrylic tank are filled with phase change material (PCM).

PCM filling process was carried out from the top of tank, and then, acrylic lid was bolted back in place. Four thermocouple probes (PT100) were inserted in the different locations as shown in Fig. 1 in the storage tank through compression fittings on the outside of the PCM container to measure temperatures of PCM. Out of these, the two thermocouples (TC3 and TC4) are inserted from top in vertical position and two (TC5 and TC6) from side of the tank in horizontal position. Additional two thermocouple probes (PT100) were inserted at inlet (TC1) and outlet (TC2) pipes of storage tank in order to measure temperature of HTF. The thermocouples are connected to a temperature indicator which provides instantaneous digital outputs. All the thermocouples are calibrated in the laboratory with the help of temperature trainer before use. The storage tank is insulated in order to reduce heat losses. A 3.85-kg commercial grade paraffin wax white is used as PCM. Paraffin wax is chemically indicated as hydrocarbons with general formula C_nH_{2n+2}, and commercially available laboratory used wax is reported here in finding. The thermophysical properties of paraffin wax used are indicated in Table 1, where melting point, density, latent heat of fusion, and specific heats are taken from supplier reference values. The thermal conductivity of paraffin wax values used is benchmarked by Farid (2004) and is not separately measured. Water is used as heat transfer fluid.

The hot water bath at constant temperature and pressure head is used to supply the hot water (HTF) inside the copper pipe which is passes through the storage tank during the charging process. In this process, PCM absorbs heat from hot water. Electric heater is used to heat the water in

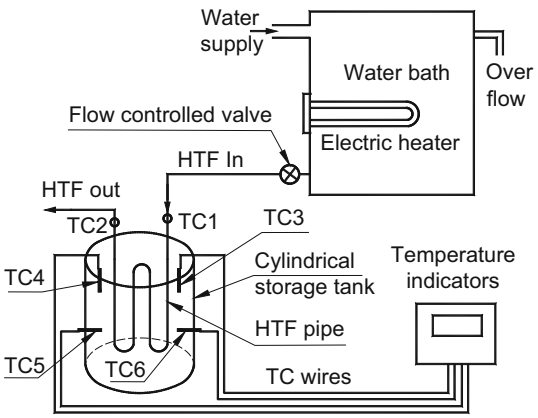

Fig. 1 Schematic diagram of the experimental setup

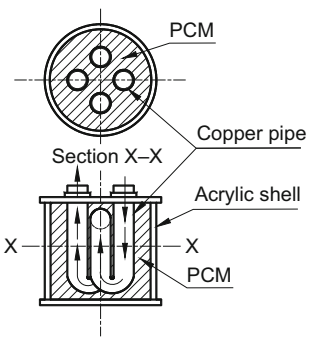

Fig. 2 Storage tank

Table 1 Thermophysical properties of commercial grade organic paraffin wax white

Melting temperature	50 °C
Density	950 kg m^{-3}
Latent heat of fusion	185 kJ kg^{-1}
Specific heat (solid)	2.4 kJ kg^{-1} K^{-1}
Specific heat (liquid)	2.45 kJ kg^{-1} K^{-1}
Thermal conductivity (liquid)	0.167 W m^{-1} K^{-1} [3]
Volume taken for study	~4 L

the water bath. The immersion heater is connected with a bulkhead fitting to the hot water bath. One-liter measuring flask and stop watch are used to measure the flow rate of HTF. For the discharging process, the same water bath is used to supply the cold water. The throttling valve is provided in the HTF flow line to control the flow rate of water.

Experimental run

A series of melting and solidification experiments were conducted to study the effect of mass flow rate of HTF on thermal behavior of the PCM. At beginning of the experiment, paraffin wax was solid in the cylindrical shell. A hot water at constant flow rate from the constant temperature bath was made to flow into the copper pipe by static head between heat exchanger and hot water bath. During charging, the PCM gets heated up to melting temperature (storing the energy as sensible heat). Later heat is stored as latent heat once the PCM melts and becomes liquid. The energy is then stored as sensible heat in liquid PCM. Temperatures of the PCM and HTF were recorded at intervals of 15 min. The charging process was continued until the all PCM completely melted. The temperatures of the HTF at inlet and outlet are recorded. Also the temperatures of the PCM at four locations are recorded. During discharging (solidification), cold water was used to circulate through copper pipe. All the temperatures were recorded at intervals of 5 min.

Result and discussion

The temperatures of PCM at different location in the storage tank and temperature of HTF at inlet and outlet are recorded during melting and during solidification under the different HTF mass flow rates from 35 to 75 LPH with increment 5 LPH. The total heat available, total heat storage, and system efficiency of process are computed during both charging and discharging processes.

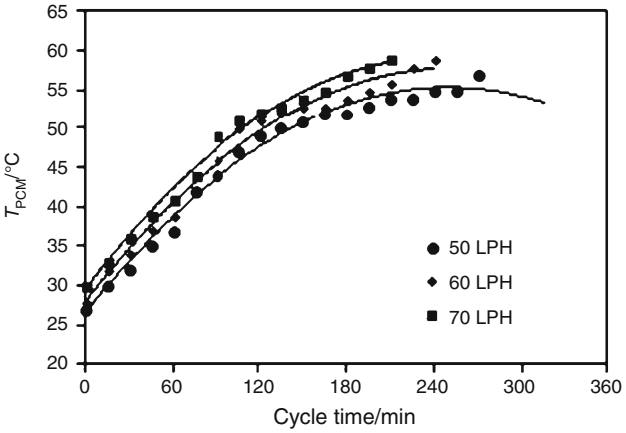

Fig. 3 Effect of mass flow rate on temperature of PCM and cycle time

Charging leading to melting of PCM

The effect of HTF flow rate on average PCM temperature during the charging process is shown in Fig. 3. The inlet HTF temperatures were in the range 65 ± 2 °C.

Under different HTF flow rates, the trend of the PCM temperature with time is found as follows:

$$T_{PCM} = 26.42 + 0.231t - 4.2 \times 10^{-4} t^2 \quad \text{and} \quad R^2 = 0.989 \quad \text{for} \quad 50 \text{ LPH} \tag{6}$$

$$T_{PCM} = 27.86 + 0.236t - 4.4 \times 10^{-3} t^2 \quad \text{and} \quad R^2 = 0.986 \quad \text{for} \quad 60 \text{ LPH} \tag{7}$$

$$T_{PCM} = 29.45 + 0.243t - 4.9 \times 10^{-3} t^2 \quad \text{and} \quad R^2 = 0.992 \quad \text{for} \quad 70 \text{ LPH} \tag{8}$$

The trend lines of PCM temperatures at all flow rates are quite similar during the charging. The correlation coefficient R^2 for all flow rates are about +1. That indicates the perfect positive polynomial relationship between PCM temperature (T_{PCM}) and charging time (t). In the initial stage, the PCM temperature rapidly rises within 120 min. This is due to sensible heating of PCM. In the second stage, PCM temperature is nearly constant marking latent heating resulting phase change. During the last stage of charging, heating of PCM liquid shows a rapid change in temperature compared to second stage isothermal melting. It is found that PCM completely melted within about 315 min under various flow rates.

Figure 4 shows the effect of varying the mass flow rates on the charging cycle time of PCM storage tank. It is clear from result that the charging time is reduced with increasing the flow rate; it is maximum as 310 min for 35 LPH and minimum as 195 min for 80 LPH.

The cycle time and flow rate relationship is represented by

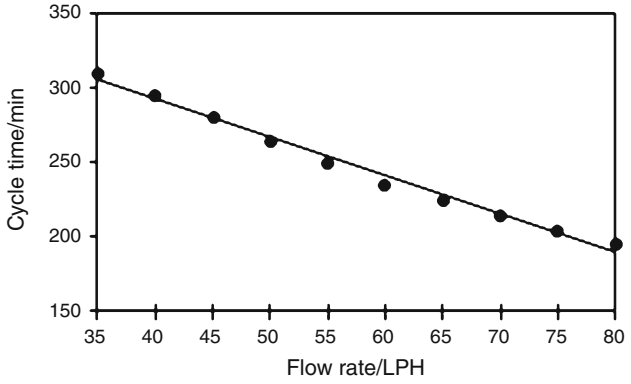

Fig. 4 Effect of mass flow rate on cycle time

$$t = 395.6 + 2.575m_{\mathrm{w}} \tag{9}$$

The correlation coefficient $R^2 = 0.99$ indicates that cycle time strongly follows linear relationship with flow rate as above equation.

The comparison between energy storage and energy available for different flow rates is shown in Fig. 5. It is found that energy available at higher flow rate is higher but there is no much variation in energy storage. The rate of increasing available energy is greater than that of stored energy. Therefore, the storage efficiency is decreased with increase in mass flow rate as shown in Fig. 6.

The correlation of energy storage or energy available with flow rates is given by

$$Q_{\mathrm{A}} = 251.3 + 37.27m_{\mathrm{w}} \quad \text{and} \quad R^2 = 0.992 \tag{10}$$

$$Q_{\mathrm{PCM}} = 979.0 + 0.028m_{\mathrm{w}} \quad \text{and} \quad R^2 \approx 0 \tag{11}$$

The coefficient of correlation in case of energy storage and flow rates is 0 (i.e., $R^2 \approx 0$), meant that there is no much variation in energy storage with flow rate of HTF.

The correlation of energy storage efficiency with flow rates is given by

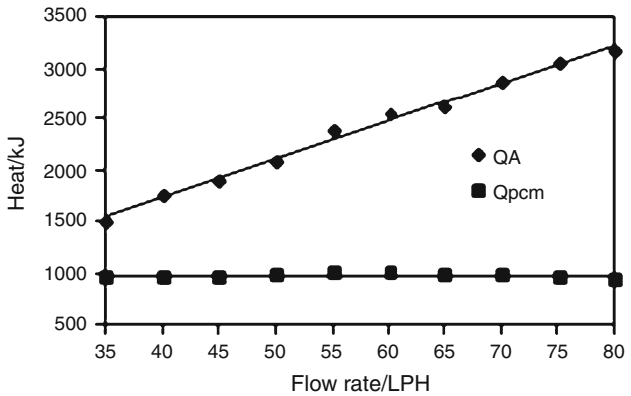

Fig. 5 Effect of flow rates on energy stored (Q_{pcm}) and energy available (Q_{A})

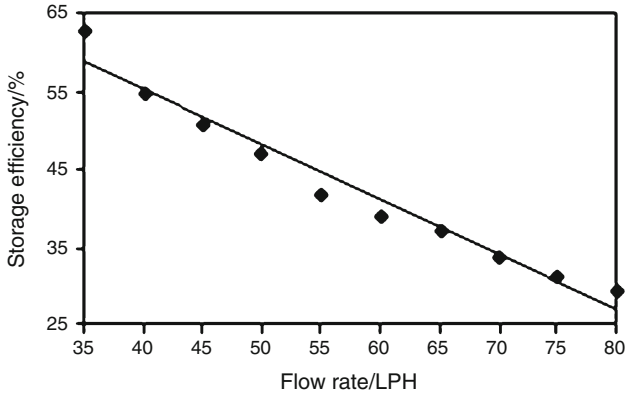

Fig. 6 Effect of flow rates on energy storage efficiency

$$\eta = 83.50 - 0.702m_{\mathrm{w}} \quad \text{and} \quad R^2 = 0.964 \tag{12}$$

Discharging leading to solidification of PCM

The effect of HTF flow rate on average PCM temperature during the discharging process is shown in Fig. 7. It is observed that the solidification processes is much faster than the melting process. HTF absorbs heat with faster rate compared to heat absorb by PCM during the charging.

Under different HTF flow rates, the trend of the PCM temperature with time is found as follows:

$$T_{\mathrm{PCM}} = 58.16 - 0.271t - 2 \times 10^{-3}t^2 \quad \text{and} \quad R^2 = 0.988 \quad \text{for} \quad 50\ \text{LPH} \tag{13}$$

$$T_{\mathrm{PCM}} = 57.17 - 0.287t - 2 \times 10^{-3}t^2 \quad \text{and} \quad R^2 = 0.982 \quad \text{for} \quad 60\ \text{LPH} \tag{14}$$

$$T_{\mathrm{PCM}} = 58.44 - 0.288t - 6 \times 10^{-3}t^2 \quad \text{and} \quad R^2 = 0.985 \quad \text{for} \quad 70\ \text{LPH} \tag{15}$$

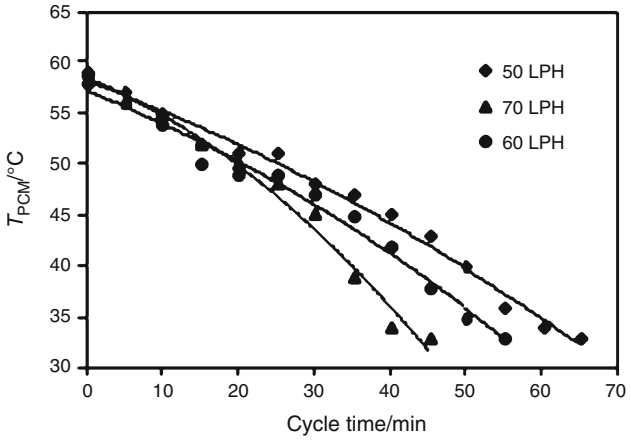

Fig. 7 Effect of mass flow rate on temperature of PCM during solidification

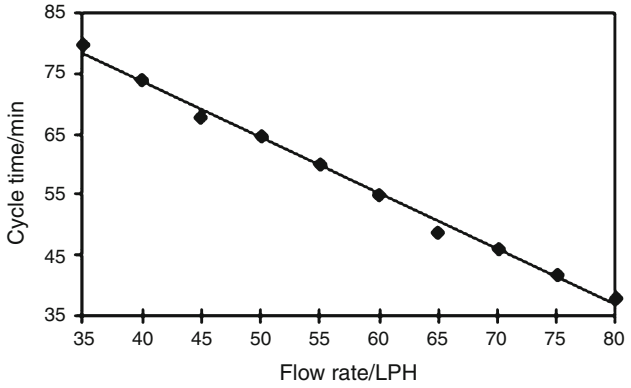

Fig. 8 Effect of mass flow rate on solidification cycle time

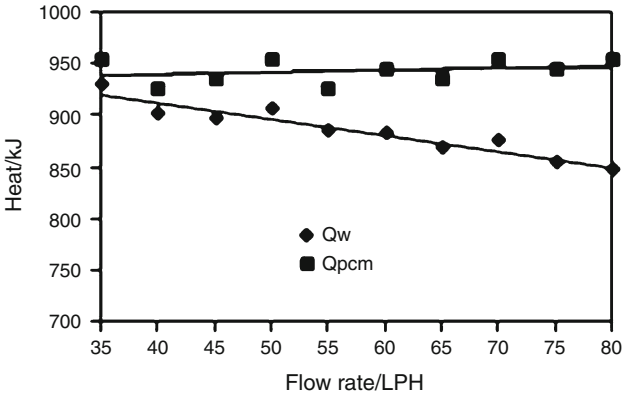

Fig. 9 Effect of flow rates on heat available (Q_{PCM}) and heat absorbed by water (Q_W)

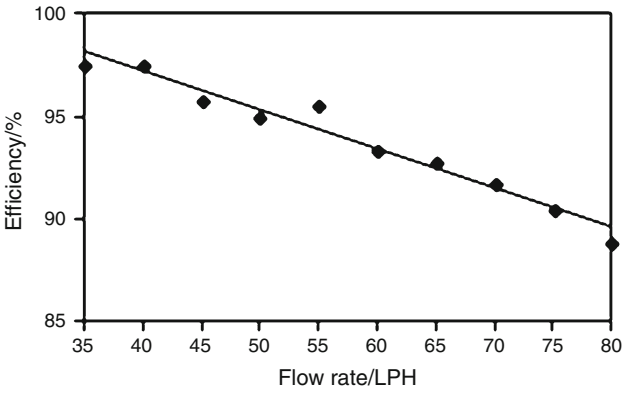

Fig. 10 Effect of mass flow rates on heat release efficiency

The trend lines of PCM temperatures at all flow rates are quite similar during the discharging. The correlation coefficient R^2 for all flow rates are about +1. That indicates the perfect positive polynomial relationship between PCM temperature (T_{PCM}) and discharging time (t).

Figure 8 shows the discharging cycle time for different flow rates. Under various flow rates, PCM solidifies within time 80 min. For 35 LPH, it solidified within the 35 min in contrast it requires 195 min to melt. It is due to crystallization cracks formed during solidification while during melting it was getting filled by molten material. This explains the transient behavior while discharging.

The cycle time and flow rate relationship is represented by

$$t = 111.0 - 0.927 m_w \tag{16}$$

The correlation coefficient $R^2 = 0.995$ indicates that cycle time strongly follows linear relationship with flow rate.

The heat available and heat absorbed by water in discharging process at different mass flow rates are shown in Fig. 9. The correlation is given by

$$Q_w = 930.2 + 0.226 m_w \quad \text{and} \quad R^2 = 0.088 \tag{17}$$

$$Q_{PCM} = 976.4 - 1.589 m_w \quad \text{and} \quad R^2 = 0.908 \tag{18}$$

The efficiency of discharging processes corresponding mass flow rates is shown in Fig. 10. The correlation of discharging efficiency with flow rates is given by

$$\eta = 104.7 - 0.189 m_w \quad \text{and} \quad R^2 = 0.960 \tag{19}$$

Uncertainty analysis

Least count of instruments used in experiment indicates the uncertainty in the direct measurement and same is used to report the calculation uncertain in parameters using the method of error propagation. Uncertainties in measurement of temperature is in order of $U_T = \pm 0.02$ °C for thermocouples, ±0.001 kg for mass of water, and ±1 s for time.

Uncertainties in calculated parameters are calculated using following relationship:

$$m_w = f(V, t) \quad \text{and} \quad U_{m_w} = \sqrt{\left(\frac{\partial m_w}{\partial V}\right)^2 U_V^2 + \left(\frac{\partial m_w}{\partial t}\right)^2 U_t^2} \tag{20}$$

$$Q_A = f(m_w, T, t) \quad \text{and}$$
$$U_{Q_A} = \sqrt{\left(\frac{\partial Q_A}{\partial m_w}\right)^2 U_{m_w}^2 + \left(\frac{\partial Q_A}{\partial T}\right)^2 U_t^2 + \left(\frac{\partial Q_A}{\partial t}\right)^2 U_t^2} \tag{21}$$

$$Q_{PCM} = f(M_{PCM}, T_1, T_2) \quad \text{and} \quad U_{Q_{PCM}} =$$
$$\sqrt{\left(\frac{\partial Q_{PCM}}{\partial M_{PCM}}\right)^2 U_{M_{PCM}}^2 + \left(\frac{\partial Q_{PCM}}{\partial T_1}\right)^2 U_{T_1}^2 + \left(\frac{\partial Q_{PCM}}{\partial T_2}\right)^2 U_{T_2}^2} \tag{22}$$

Table 2 Uncertainties in calculated parameters

Flow rate/LPH	Uncertainty/%			
	U_{mw}	U_{QA}	U_{QPCM}	U_{η}
50	1.39	1.65	0.26	1.67
60	1.67	1.84	0.26	1.86
70	1.96	2.10	0.26	2.11

$$\eta = f(Q_{PCM}, Q_A) \quad \text{and}$$
$$U_{\eta} = \sqrt{\left(\frac{\partial \eta}{\partial Q_{PCM}}\right)^2 U_{Q_{PCM}}^2 + \left(\frac{\partial \eta}{\partial Q_A}\right)^2 U_{Q_A}^2} \tag{23}$$

Table 2 provides the uncertainties in calculated parameters narrowing exceeding 2 %.

Conclusions

The work reports experimental thermal behavior response of paraffin wax as storage unit with various mass flow rates in shell and tube of four passes as under:

- The trends of temperature change are quite similar under various HTF flow rates during melting and solidification. In the initial stage of charging and discharging, the PCM temperature rapidly rises and attains steadiness after 120 min.
- There is not much variation in heat energy storage by PCM during melting and amount of heat release during solidification under the different mass flow rates of HTF as it had constant mass of PCM. However, the charging and discharging time are reduced from 310 to 195 min and from 80 to 38 min, respectively, with increase in flow rate of HTF from 35 to 75 LPH.
- Time required for solidification is about 20–25 % of required while melting. This is due to higher temperature difference available for heat transfer during discharging process and fissure formed while solidification helps in quick release of energy.
- The efficiencies of heat release during discharging are higher than that of heat storage during charging. The efficiencies of heat storage during charging is reduced from 63 to 30 % and efficiency of heat release during discharging reduced from 97 to 89 % with increase in flow rates of HTF from 35 to 80 LPH.

The present work provides guidelines for modeling thermal performance of paraffin wax as low-temperature latent heat energy storage. The performance of paraffin wax with respect to mass flow rate of HTF provides behavior of paraffin wax at variable intensity which can be used to increase the availability energy for low-temperature application as in case of domestic solar water heater. Further, it is concluded that the paraffin wax four-pass tube storage unit is more favorable than single-pass large-diameter tube unit because multi-pass storage unit have larger heat transfer surface area.

Acknowledgements Contribution to the development and fabrication of experimental setup by students Bhavesh, Tanuj, Ankit, and Dharmesh is acknowledged.

References

1. Sharma A, Tyagi VV, Chen CR, Budhi D. Review on thermal energy storage with phase change materials and applications. Ren Sust Energy Rev. 2009;13:318–45.
2. Al-Abidi AA, Mat SB, Sopian K, Sulaiman MY, Lim CH, Th A. Review of thermal energy storage for air conditioning systems. Ren Sust Energy Rev. 2012;16:5802–19.
3. Farid MM, Khudhair AM, Razack SAK, Al-Hallaj S. A review on phase change energy storage: materials and applications. Energy Conv Mana. 2004;45:1597–615.
4. Tyagi VV, Pandey AK, Kaushik SC, Tyagi SK. Thermal performance evaluation of a solar air heater with and without thermal energy storage. J Therm Anal Calorim. 2012;107(3):1345–52.
5. Jeon Jisoo, Lee Jung-Hun, Seo Jungki, Jeong Su-Gwang, Kim Sumin. Application of PCM thermal energy storage system to reduce building energy consumption. J Therm Anal Calorim. 2013;111(1):279–88.
6. Yuan Yanping, Zhang Nan, Tao Wenquan, Cao Xiaoling, He Yaling. Fatty acids as phase change materials: a review. Ren Sust Energy Rev. 2014;29:482–98.
7. Liu Ming, Saman Wasim, Bruno Frank. Review on storage materials and thermal performance enhancement techniques for high temperature phase change thermal storage systems. Ren Sust Energy Rev. 2012;16:2118–32.
8. Jankowski NR, McCluskey FP. A review of phase change materials for vehicle component thermal buffering. Appl Energy. 2014;113:1525–61.
9. Harikrishnan S, Deepak K, Kalaiselvam S. Thermal energy storage behavior of composite using hybrid nano-materials as PCM for solar heating systems. J Therm Anal Calorim. 2014;115(2):1563–71.
10. Rathod MK, Banerjee J. Thermal stability of phase change materials used in latent heat energy storage systems: a review. Ren Sust Energy Rev. 2013;18:246–58.
11. Li Min, Zhishen Wu. Thermal properties of the graphite/nodocosane composite PCM. J Therm Anal Calorim. 2013;111(1):77–83.
12. Jeong Su-Gwang, Jeon Jisoo, Chung Okyoung, Kim Sughwan, Kim Sumin. Evaluation of PCM/diatomite composites using exfoliated graphite nano-platelets to improve thermal properties. J Therm Anal Calorim. 2013;114(2):689–98.
13. Parameshwaran R, Jayavel R, Kalaiselvam S. Study on thermal properties of organic ester phase-change material embedded with silver nano-particles. J Therm Anal Calorim. 2012;114(2):845–58.
14. Wang N, Zhang XR, Zhu DS, Gao JW. The investigation of thermal conductivity and energy storage properties of graphite/paraffin composites. J Therm Anal Calorim. 2012;107(3):949–54.

15. Anghel EM, Georgiev A, Petrescu S, Popov R, Constantinescu M. Thermo-physical characterization of some paraffins used as phase change materials for thermal energy storage. J Therm Anal Calorim. 2014;117(2):557–66.
16. Murray R, Desgrosseilliers L, Stewart J, Osbourne N, Marin G, Safatli A, Groulx D, White MA. Design of a latent heat energy storage system, solar thermal application. World Renewable Energy Congress, 8–13 May 2011, Linkoping, Sweden; 3757–64.
17. Ge H, Li H, Mei S, Liu J. Low melting point liquid metal as a new class of phase change material. Ren Sustain Energy Rev. 2013;21:331–46.
18. Akgun M, Aydin O, Kaygusuz K. Experimental study on melting/solidification characteristics of paraffin as PCM. Energy Cons Man. 2007;48:669–78.
19. Benmansour A, Hamdan MA, Bengeuddach A. Experimental and numerical investigation of solid particles thermal energy storage unit. Appl Therm Eng. 2006;26:513–8.
20. Groulx D, Ogoh W. Solid liquid phase change simulation applied to a cylindrical latent heat energy storage system. Proceedings of the COMSOL conference 2009, Boston; 2009.
21. Hasan A. Phase change material energy storage system employing palmitric acid. Sol Energy. 1994;52:143–54.